water

MDPI

Article

Adsorption of Ibuprofen from Water Using Banana Peel Biochar: Experimental Investigation and Machine Learning Algorithms

Md. Rezwanul Islam [1,2,*], Qingyue Wang [1,*], Sumaya Sharmin [1,2] and Christian Ebere Enyoh [1]

[1] Graduate School of Science and Engineering, Saitama University, 255 Shimo-Okubo, Sakura-ku, Saitama 338-8570, Japan; sumayabau@gmail.com (S.S.); cenyoh@gmail.com (C.E.E.)
[2] Department of Agricultural Extension, Khamarbari, Dhaka 1215, Bangladesh
* Correspondence: rezwandae@gmail.com (M.R.I.); seiyo@mail.saitama-u.ac.jp (Q.W.)

Abstract: Ibuprofen is a significant nonsteroidal anti-inflammatory drug that poses environmental and health risks when present in wastewater because of its persistence and probable toxicity. This study investigates the use of banana peel biochar (BPB) made at 600 °C to 900 °C to eliminate ibuprofen from aqueous solutions. The uniqueness of this work lies in the high-temperature pyrolysis process, which has not been previously explored for the ibuprofen removal efficiency using BPB. The batch experiment was conducted considering initial concentrations, pH, and contact time. The data were compared with different algorithms, with Linear Regression (LR), Support Vector Machines (SVM), Decision Trees (DT), Random Forest (RF), and k-Nearest Neighbor (k-NN) to forecast the performance. The results revealed that banana peel biochar at 900 °C exhibited the highest ibuprofen removal efficiency (69.28 ± 0.83%) at 125 mg/L concentration with the sequence of BPB900 > BPB800 > BPB700 > BPB600. A maximum removal efficiency of 72.67 ± 0.75% was observed at pH 9. Adsorption behavior was analyzed using isotherm and kinetic models, with the Freundlich isotherm model (R^2 value 0.9620) indicating heterogeneous adsorption and the pseudo-second-order (PSO) kinetic model (R^2 value 0.9969) suggesting that physicochemical interactions govern the process. FTIR analysis ensured the existence of functional groups (hydroxyl, carboxylic, carbonyl, and aromatic rings) responsible for adsorption. Machine learning algorithms, especially RF, demonstrated outstanding performance with 90.07% accuracy in predicting the experimental data. In comparison to other adsorbents, BPB demonstrated superior removal efficiency, underscoring its effectiveness. The study suggests that BPB, particularly at 900 °C, is effective in removing ibuprofen, and due to its sustainable production, it offers a potential solution for wastewater treatment.

Keywords: ibuprofen elimination; banana peel-derived adsorbent; sorption isotherm; kinetic model; computational learning

check for updates

Citation: Islam, M.R.; Wang, Q.; Sharmin, S.; Enyoh, C.E. Adsorption of Ibuprofen from Water Using Banana Peel Biochar: Experimental Investigation and Machine Learning Algorithms. *Water* **2024**, *16*, 3469. https://doi.org/10.3390/w16233469

Received: 30 October 2024
Revised: 29 November 2024
Accepted: 30 November 2024
Published: 2 December 2024

Copyright: © 2024 by the authors. Licensee MDPI, Basel, Switzerland. This article is an open access article distributed under the terms and conditions of the Creative Commons Attribution (CC BY) license (https://creativecommons.org/licenses/by/4.0/).

1. Introduction

Water pollution is an escalating global concern, leading to widespread impacts on ecosystems and human health and contributing to an increasing scarcity of clean water [1]. The pollution has been exacerbated by the widespread presence of pharmaceutical products in ecosystems worldwide [2–4]. Environmental scientists are particularly alarmed by various medical effluents containing nonsteroidal anti-inflammatory drugs like ibuprofen, naproxen, diclofenac, and ketoprofen. Among these, ibuprofen (2-[4-(2-Methylpropyl)phenyl]propanoic acid) stands out as one of the most commonly prescribed drugs, primarily used to alleviate pain, tissue inflammation, and fever [5]. It is also recommended for conditions like rheumatoid arthritis, osteoarthritis, and tendonitis. Annually, approximately 200 tons of ibuprofen are consumed globally [6]. A significant quantity of ibuprofen has been detected (up to 25 mg/L) in wastewater treatment plant effluents and river water in many countries [7]. Its presence has been linked to phytoplankton toxicity and damage to the gills and kidneys of fish [8]. Long-term exposure to ibuprofen can lead

to health complications in humans, including kidney and liver issues [9], as well as gastrointestinal and cardiovascular problems such as myocardial infarction and sudden cardiac arrest (heart failure) [10]. Approximately 69% of the ibuprofen excreted from the human body undergoes hydroxylation and carboxylation processes, resulting in metabolites that pose even greater toxicity compared to the original compound [11].

Different methods like adsorption [12], flocculation or coagulation [13], filtration [14], ion exchange [15], degradation [16], chemical oxidation [17], advanced oxidation processes [18], biological treatment [19], and the Fenton process [20] have been used to remove pharmaceutical compounds from various sources. Among all these methods, adsorption has garnered noteworthy interest because of its ease, cost-efficacy, high efficiency, and reproducibility [21,22]. In the adsorption process, diversified adsorbents are employed, including plant biomasses and inorganic materials [23,24].

Bananas (*Musa acuminata*) are the second most widely cultivated fruit globally. In 2022, banana production reached 135.11 million tons, with banana peels (BP)—constituting 30–40% of the fruit's total weight—resulting in approximately 54 million tons of waste annually [25]. This biomass is largely underutilized and often discarded as waste [26], releasing greenhouse gases and toxic compounds during decomposition [27]. In the pursuit of sustainable environmental management and efficient resource utilization, banana peel biochar has emerged as a promising adsorbent for various contaminants, including heavy metals, phenolic compounds, organic acids, pesticides, medical contaminants, and aflatoxins [28–31]. Banana peel was chosen as a biochar source owing to its minimal cost, easy availability, and effective adsorption capacity, stemming from its high cellulose and pectin content, which generate a carbon material with an extensive surface area and functional groups that enhance adsorption [32]. Although different adsorbents have been investigated for ibuprofen removal from wastewater, including French plane tree leaves biochar [33], pepper stem biochar [34], pine wood biochar [35], and walnut shell biochar [36], banana peel biochar has not been explored for this purpose.

The incorporation of machine learning algorithms in adsorption studies influences their ability to model and predict complex interactions between multiple variables, such as contaminant concentration and pH, which are difficult to fully explore through traditional batch experiments alone. Machine learning can analyze large datasets from these experiments, uncovering patterns and relationships that conventional statistical analyses might miss. The machine learning algorithms used each offer distinct advantages: LR models linear data relationships; RF provides accurate, interpretable predictions and minimizes overfitting; SVM excels in high-dimensional spaces with high accuracy but requires careful tuning; DT handles non-linear data and missing values but can overfit; and k-NN is intuitive for classification and regression, though sensitive to noise and high dimensionality [37–39]. This leads to more accurate predictions of adsorption behavior in real-world environmental systems with variable and complex conditions. By using machine learning, adsorption processes can be optimized, improving efficiency and enabling more informed decisions in environmental management.

The originality of this research lies in evaluating banana peel biochar, which has not been previously considered for ibuprofen removal from wastewater. Furthermore, the investigation applies machine learning algorithms to predict adsorption outcomes based on batch adsorption experiments (pH, initial concentration, shaking speed, contact time, and removal efficiency), introducing an innovative approach to optimizing the removal process. Therefore, this study is focused on addressing these gaps by conducting batch adsorption of ibuprofen using banana peel biochar and comparing it with a machine learning algorithm for better prediction.

2. Materials and Methods

2.1. Materials and Chemicals

Banana (*Musa acuminata*) was bought from Maruetsu Super Shop (35.8678° N, 139.6089° E) in Saitama, Japan. After eating, the banana peel was dried. Subsequently, the peel was ground and sieved with a 0.25 MF sieve.

The chemical solutions, including 10% hydrochloric acid (36%) and sodium hydroxide (97%), were delivered by Wako Pure Chemical Industries, while ibuprofen ($C1_3H_{18}O_2$), sodium chloride (99.5%) and ethanol (99.5%) were obtained from Fujifilm Wako Pure Chemical Corporation. Argon (Ar), with a purity of 99.9995%, sourced from Suzuki Shokan Co., was utilized as an inert gas during the experiment. Ultrapure (Type1) water (produced from Direct-Q® 3 UV Water Purification System) was used to prepare the solutions during the experiment and rinse after washing the glassware.

2.2. Preparation of Adsorbents

The ground banana peel (5 g) undertook a pyrolysis process within a fixed-bed reactor. This process involved placing the banana peel powder in the reactor and heating it to temperatures ranging from 600 °C to 900 °C, with a 10 °C per minute rate. The sample was held at the concerned temperature for 30 min. To maintain an inert atmosphere, argon gas was introduced with a 100 mL/min flow rate following the method of the author's previous study [40]. After the pyrolysis, the resulting biochar was retrieved from the tube once it had cooled. As a result, biochar adsorbents—BPB600, BPB700, BPB800, and BPB900—were produced at 600 °C, 700 °C, 800 °C, and 900 °C, respectively. The final product, the biochar with 100 µm particle size, was then stored in a sealed aluminum bag to maintain the quality during analysis.

2.3. Characterization of Adsorbents

2.3.1. Morphological Characterization

The morphological features of banana peel biochar were analyzed using scanning electron microscopy (SEM) with the SU1510 instrument. The specific surface area and pore size distribution were measured considering N_2 adsorption–desorption isotherms at −196 °C (BELSORP-miniX-TKS0, MicrotracBEL Corp., Osaka, Japan) under a relative pressure of P/P_0 0.995. Total pore volume was derived from N_2 adsorption isotherms at P/P_0 0.990. The specific surface area and micropore volume were measured using the Brunauer–Emmett–Teller (BET) equation and t-plot method, respectively. Additionally, micropore size distribution was assessed using the MP method, while mesopore size distribution was evaluated considering the Barrett–Joyner–Halenda method.

2.3.2. Chemical Characterization

Fourier Transform Infrared spectroscopy (FTIR) was performed to recognize the functional groups present in the biochar. The FTIR analysis utilized the IR-6100 apparatus from JASCO Co., Ltd., Hachioji, Tokyo, Japan, following the method used by Islam et al. [40]. X-ray photoelectron spectroscopy (XPS) was used to examine the chemical composition of the surface. The XPS spectra were obtained using a monochromatic Al Kα radiation source, with binding energies calibrated to the peak.

2.4. Batch Experiments

Batch experiments were accomplished using 20 ± 0.1 mg banana peel biochar at room temperature using BPB600, BPB700, BPB800, and BPB900. Various initial concentrations of ibuprofen (25, 50, 75, 100, 125, and 150 mg/L) were used to investigate the effect of concentration on the adsorption. As ibuprofen is poorly soluble in water, 30% ethanol was used to prepare the ibuprofen solutions during the experiment. Additionally, various contact times (30, 60, 90, 120, and 240 min) were investigated, considering BPB900 adsorbent with a 125 mg/L initial concentration because of higher adsorption capacity compared to BPB600, BPB700, and BPB800.

The effect of pH was evaluated using various pH levels (3, 5, 7, 9, and 11) in combination with banana peel biochar (900 °C) and an ibuprofen concentration of 125 mg/L. The solutions were sealed tightly and agitated in a shaker at a constant speed of 200 rpm for 1 h. Subsequently, the samples obtained from the batch adsorption experiments underwent filtration using a 0.45 µm membrane. The absorbance of ibuprofen was measured at λ_{max} = 270 nm with the help of a UV-VIS spectrophotometer (UVmini-1240, Shimadzu, Japan). For determination of the point of zero charge (pH_{zpc}), nine 0.01 M NaCl solutions were made with pH 3, 5, 7, 9, and 11, each replicated three times. Banana peel biochar (20 mg), pyrolyzed at 900 °C, was mixed into each solution, which was then shaken at 200 rpm for 1 h to allow equilibrium to be reached. The final pH was determined afterward. By plotting the change in pH (ΔpH = final pH − initial pH) against the initial pH, the pH_{zpc} is found where ΔpH equals zero. We followed the method described by Islam et al. [41].

The assessment of ibuprofen removal efficiency (%) and adsorption capacity (mg/g) was conducted based on the following equations [42]:

$$\text{Removal efficiency}(\%) = \frac{Co - Ce}{Co} \times 100 \quad (1)$$

$$\text{Adsorption capacity}\left(\frac{mg}{g}\right) = \frac{(Co - Ce) \times V}{M} \quad (2)$$

where Co (mg/L) and Ce (mg/L) are the concentrations of ibuprofen at the initial and equilibrium levels. On the other hand, M (mg) is the adsorbent mass, and V (mL) signifies the ibuprofen solution volume.

2.5. Regeneration Study

The regeneration study was conducted using 150 mg of BPB900 in 50 mL of an ibuprofen solution (125 mg/L) at room temperature, following the method of Yudha et al. [43]. The solution was shaken for 1 h, then filtered, and the absorbance of the filtrate was measured with the help of a UV spectrophotometer. The filter paper was cleaned with acetone, and the adsorbent was rinsed with Milli-Q water and oven-dried at 105 °C for 1 h and 30 min. This process was repeated for four successive cycles.

2.6. Adsorption Isotherms

To describe the adsorption process, Langmuir and Freundlich adsorption isotherms were utilized. The Langmuir adsorption isotherm describes a dynamic adsorption method occurring on a uniform, non-interacting surface, which governs the molecular interactions between the adsorbent (banana peel biochar) and adsorbate (ibuprofen). The linearized form of the Langmuir isotherm equation is used by Islam et al. [41]:

$$\frac{1}{q_e} = \frac{1}{K_L q_m Ce} + \frac{1}{q_m} \quad (3)$$

In this equation, C_o is the initial concentration of the ibuprofen solution (mgL^{-1}), C_e is the concentration of the ibuprofen solution at equilibrium (mgL^{-1}), q_e is the amount of adsorbate (ibuprofen) adsorbed at equilibrium (mmg^{-1}), q_m indicates the adsorption capacity of the adsorbent (banana peel biochar) (mmg^{-1}), and K_L is the Langmuir constant, which reflects the intensity of adsorption (Lmg^{-1}).

On the contrary, the Freundlich isotherm proposes that adsorption appears on a heterogeneous surface involving a multilayer adsorption mechanism. The Freundlich equation is given by Baláž et al. [44]:

$$\ln q_e = \ln K_F + \frac{1}{n} \ln C_e \quad (4)$$

where q_e is the adsorbate amount (ibuprofen) adsorbed at equilibrium (mgg^{-1}), C_e is the concentration of the ibuprofen solution at equilibrium (mgL^{-1}), K_F is the Freundlich constant ($mg\ ^{1-(1/n)}L^{1/n}/g$), and n is the Freundlich exponent that implies the adsorption intensity.

2.7. Kinetic Models

The kinetics of the adsorption process were analyzed by Pseudo First Order (PFO) and Pseudo Second Order (PSO) models [45,46]. The PFO is a model where the rate of adsorption is proportional to the difference between the amount of adsorbate at equilibrium and the amount adsorbed at any given time. The PFO model is described by the following equation:

$$\ln(q_e - q_t) = \ln qe - k_1 t \quad (5)$$

where q_e is the quantity of ibuprofen adsorbed during equilibrium (mg/g), q_t is the adsorbed ibuprofen at t time (mg/g), and k_1 is the PFO rate constant (min^{-1}).

On the other hand, the PSO is a model where the adsorption rate is proportionate to the square of the amount of adsorbate adsorbed at any given time. This model indicates that adsorption occurs on the surface of identical sites. The PSO model is represented by the following equation:

$$\frac{t}{q_e} = \frac{1}{k_2 {q_e}^2} + \frac{1}{q_e} \quad (6)$$

where q_e indicates the adsorbate (ibuprofen) amount at equilibrium (mg/g), and k_2 is the rate constant of the PSO model ($gmg^{-1}min^{-1}$).

2.8. Machine Learning Algorithms

Five ML algorithms were trained to predict adsorption performance based on different independent parameters.

2.8.1. Linear Regression

Linear regression is a machine learning tool utilized to show the linear relationship between dependent and independent variables. The tool is used to predict both categorical and regressor data. This is employed to measure, explain, and predict the data [35].

2.8.2. Random Forest

Random forest is a supervised learning approach that is suitable for both classification and regression analysis. This algorithm manages large datasets efficiently, mitigates overfitting and variance, and provides easily interpretable, accurate predictions [36,37].

2.8.3. Support Vector Machines

Support Vector is a supervised learning algorithm that investigates data formulated for the analysis of regression. It shows high prediction accuracy and effectively manages high-dimensional spaces. The algorithm exhibits reduced susceptibility to overfitting and shows minimal influence from outliers [36]. However, it requires careful selection of the appropriate kernel function and poses challenges in fine-tuning.

2.8.4. Decision Trees

Decision tree is a non-linear machine learning algorithm method widely used to forecast outcomes based on trained data [47,48]. It easily handles inappropriate features, is not affected by missing values, requires no scaling, and demands minimal data preparation. However, its structure is sensitive to small changes and prone to overfitting without proper pruning and finding the optimal tree is difficult [36].

2.8.5. k-Nearest Neighbor

The k-Nearest Neighbors are the supervised learning method that handles classification and regression data. It is easy to understand but decreases significantly with data size [49]. It is sensitive to noisy data and outliers, and its performance can be challenged by high-dimensional datasets, making standardization and normalization steps essential [36].

2.9. Machine Learning Algorithms Development

The analysis aimed to predict adsorption performance using machine learning (ML) algorithms in Python within a Jupyter Notebook. Data were preprocessed by normalizing using z-score standardization to make them suitable for the algorithms. Independent and dependent variables, including pyrolysis temperature, initial concentrations, pH, shaking speed, and contact time, were standardized. Additionally, a pipeline with StandardScaler was generated for normalization. After preprocessing, the dataset was split into training (80%) and testing (20%) to assess the model's generalization capacities. The performance of these models was calculated utilizing the R-squared metric by comparing predicted values to actual performance in the test subset. To ensure robustness and mitigate overfitting, model optimization was carried out through 5-fold cross-validation, which split the training data into five subsets and validated the model.

The detailed workflow of machine learning algorithm prediction is as follows in Figure 1:

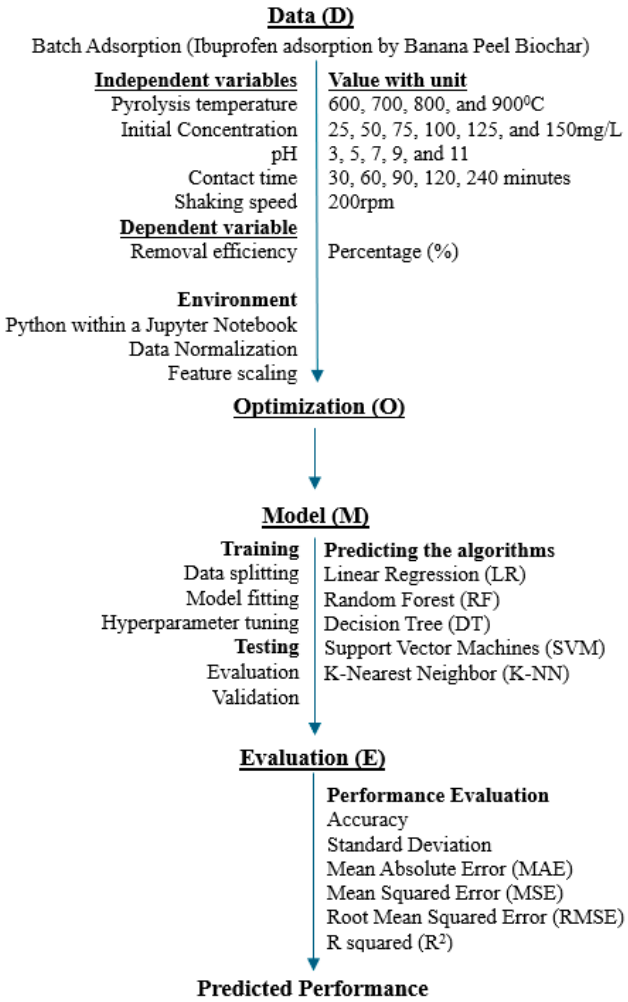


Figure 1. A flowchart for DOME recommendations in machine learning algorithm prediction.

2.10. Quality Control

The sieved sample was stored in an airtight aluminum bag. Ultrapure (Type1) water was utilized to make the solutions. The glassware used for the experiment was properly cleaned with water, sonicated, and finally rinsed with Ultrapure (Type1) water. The prepared samples were covered with aluminum foil to maintain the exact concentrations of the solution and to avoid volatilization loss of ethanol. Samples were tested three times to ensure data accuracy.

2.11. Statistical Analysis

The data were statistically analyzed using the software IBM SPSS Statistics 20, employing various statistical methodologies. Graphs were made with the help of two different software packages: OriginPro 2018 and Microsoft Office Excel.

3. Results and Discussion

3.1. Adsorbent Characterization

3.1.1. Scanning Electron Microscope (SEM) Image Analysis

The surface morphology of banana peel (BP) and its biochar was portrayed using scanning electron microscopy (SEM), as illustrated in Figure 2. SEM images revealed a highly porous, honeycomb-like structure dominated by macro-pores, with pore diameters influenced by pyrolysis temperature that is absent in raw BP. The SEM image of the BP showed fiber-like structures due to cellulose and lignin, with a compact, rough surface. The BP, which contains pectin, lignin, and other organic substances [50], develops irregular porous shapes and smooth surfaces during pyrolysis at different temperatures. This process produces smooth-edged holes, suggesting enhanced contaminant adsorption [51]. At lower temperatures, incomplete volatilization results in some residual pore space. As the temperature increases, the pores become more defined, and surface cracking may occur due to thermal decomposition. At 800 °C and 900 °C, further carbonization and structural transformation lead to a smoother and more homogeneous surface. SEM imaging provides detailed visualization of these surface changes, offering insights into the evolution of banana peel biochar morphology with varying pyrolysis temperatures. Zubair et al. [52] also noted that the highest porosity was observed in biochar derived from date palm fronds with increasing pyrolysis temperature. The porous configuration enhances adsorption capacity [36], though the adsorption also significantly depends on the functional groups present on the banana peel biochar surface [53].

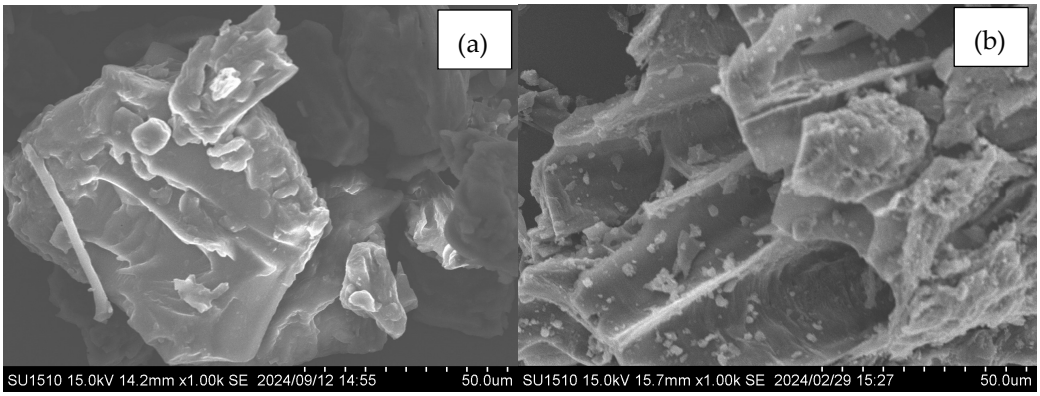


Figure 2. *Cont.*

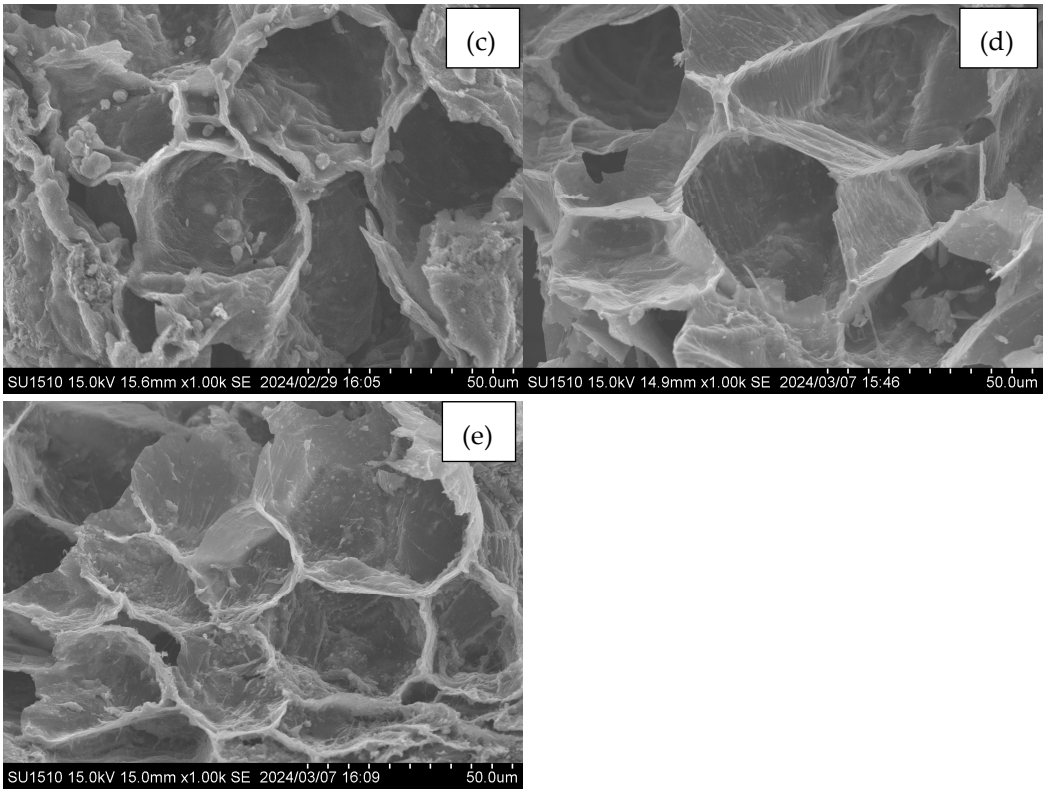


Figure 2. SEM images of (**a**) BP, (**b**) BPB600, (**c**) BPB700, (**d**) BPB800, and (**e**) BPB900, respectively.

3.1.2. Analysis of Surface Area and Porosity

The nitrogen adsorption–desorption isotherms of the banana peel biochars are mentioned in Figure 3. The graph indicated that the BPB samples show Type IV isotherms, characteristic of mesoporous materials, having a notable increase in adsorbed volume at higher relative pressures due to starting capillary condensation in mesoporous materials [54]. The sharp rise near P/P0 = 1 suggests the presence of large pores, aligning with the high mesopore volume ratios observed in the samples. A comparison was conducted by Qin et al. [55]. The BPB samples show progressive increases in specific surface area (SSA) and micropore volume (V_{mic}), though V_{mic} values remain low relative to mesopore volume (V_{meso}) with increasing pyrolysis temperature (Table S1). SSA increases notably at higher temperatures, likely enhancing surface reactivity [56]. Average pore diameter (d_{ave}) decreases with temperature, suggesting the formation of smaller, more accessible pores as pyrolysis temperature rises, favoring adsorptive performance.

3.1.3. Functional Group Analysis

The FTIR spectra of banana peel (BP) and its biochar across different temperature ranges are explained in Figure 4. The spectra reveal various peaks corresponding to different functional groups within the 400−4000 cm^{-1} region. A notable peak at around 3200−3500 cm^{-1} was connected with the O–H group. Additionally, peaks around 2931 and 2835 cm^{-1} were attributed to aliphatic stretching vibrations –CH and $–CH_2$, respectively [53,57]. The peak in the raw peel, around 2340 cm^{-1}, indicates O=C=O, which disappeared due to decomposition or volatilization during pyrolysis. This result is similar to the findings of Nguyen et al. [58], who also mentioned a peak in this region. The occurrence of peaks at 1718 cm^{-1} (related to C=O), with an additional peak at approximately 1440 cm^{-1} corresponding to the stretching vibrations of aromatic C=C [59]. Moreover, peaks at 1018 cm^{-1} represented aromatic C–O stretching vibrations. The observed shift in C–O peaks further confirmed the occurrence of aromatization with rising pyrolysis temperature [60]. The result revealed that the banana peel biochar contains a carboxylic functional group and phenol. Finally, peaks

at 839 cm^{-1} and 689 cm^{-1} were ascribed to aromatic C–H out-of-plane deformations and Si–O–Fe symmetrical stretching vibrations [30]. These findings agreed with the verdicts of Xu et al. [57], who illustrated FTIR spectra of pseudo stem biochar of bananas. Shah et al. [53] similarly reported spectra peaks for O–H stretching, C–H stretching, aromatic vibrations, Si–O stretching, and Si–O–Fe during FTIR analysis.

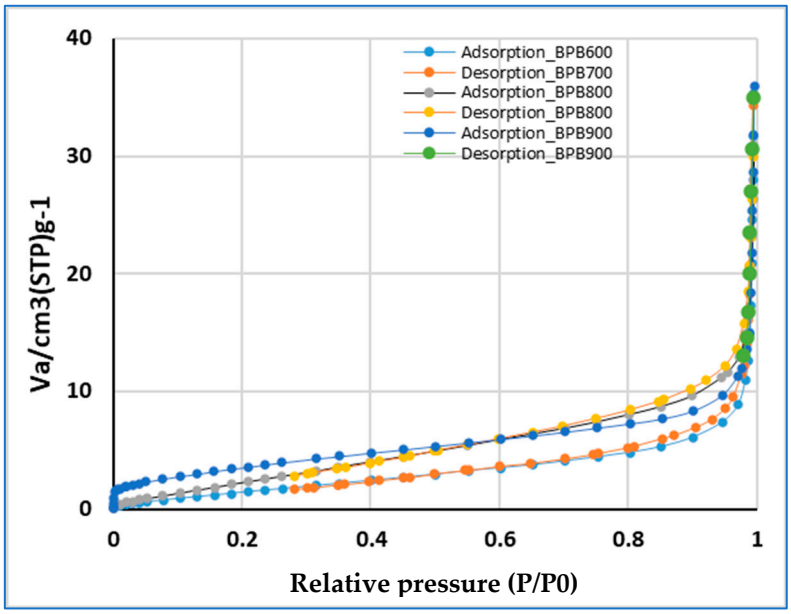


Figure 3. N_2 adsorption isotherms of BPB at different pyrolysis temperatures.

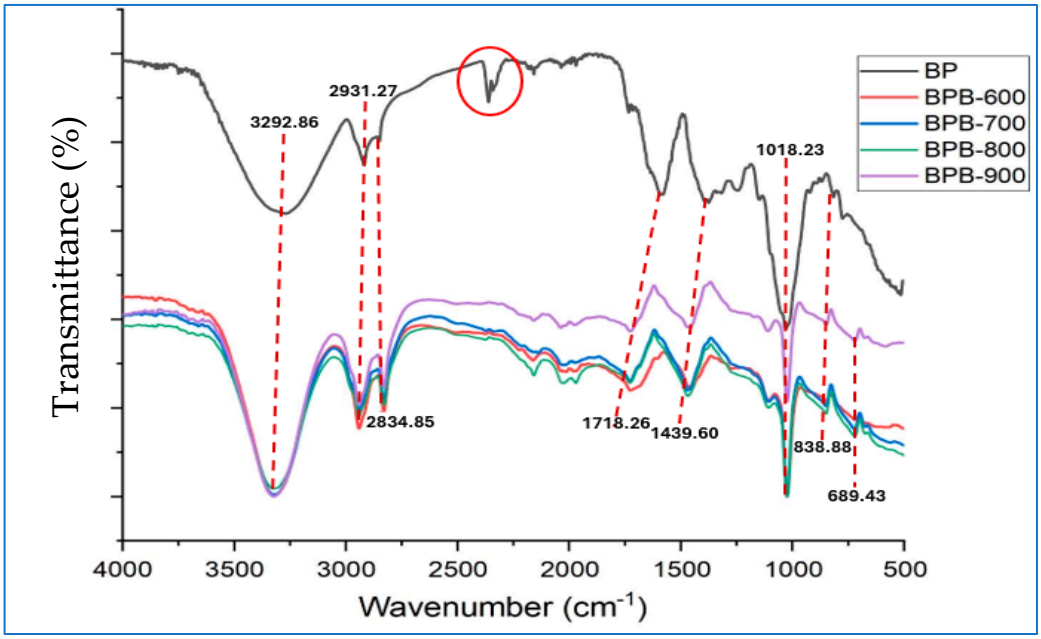


Figure 4. FTIR spectra of BP, BPB600, BPB700, BPB800, and BPB900, respectively.

3.1.4. X-Ray Photoelectron Spectroscopy (XPS) Analysis

Figure 5 indicates the XPS spectrum of the banana peel biochar. The results revealed that banana peel biochar contained a C 1s peak at 280−283 eV, revealing sp^2 hybridized carbon (C=C) from aromatic structures in biochar (Figure 5b). The second prominent peak (O 1s peak) was observed around 527–530 eV, indicating the presence of oxygen, likely from oxygen-containing functional groups in the biochar (Figure 5c). Zhang et al. [61] also reported that the C 1s and O 1s peaks were observed at nearly the same positions,

with slight differences attributed to variations in biochar synthesis conditions. In addition, the biochar possessed some other peaks of minerals like Ca, K, Mg, P, and Si [62]. The finding was comparable with the findings of the author's previous work [40], where the author characterized banana peel and found 17 different plant nutrients. Moreover, the presence of Si was justified with a peak found in FTIR spectra, where the biochar contains silicon compounds.

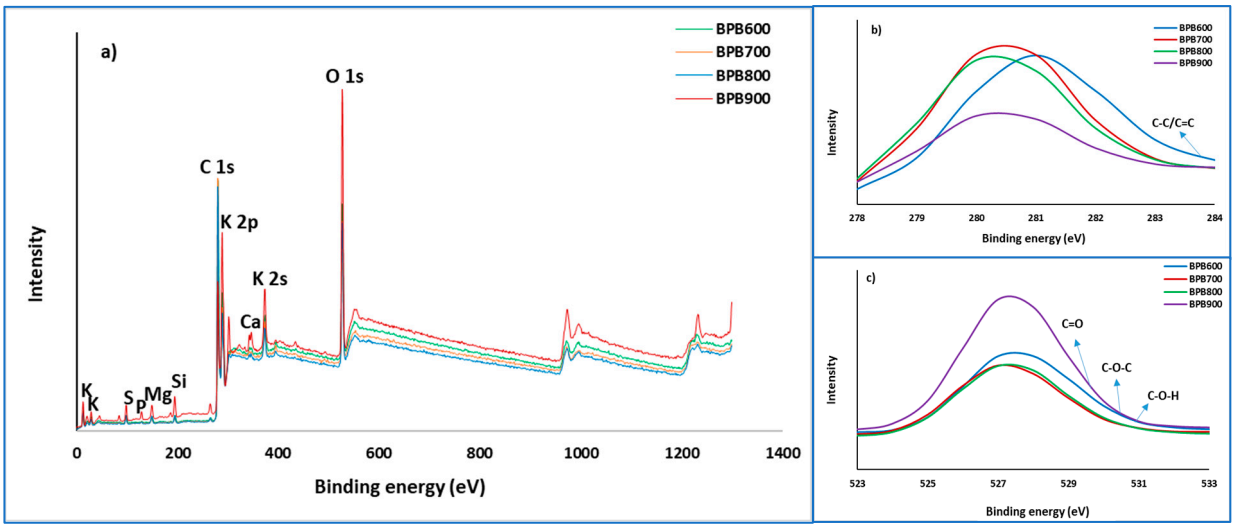


Figure 5. XPS-spectra of BPB at different temperatures (**a**); C 1s spectra of BPB (**b**); O 1s spectra of BPB (**c**).

3.2. Effect of Initial Concentrations

The removal efficiency and adsorption capacity of ibuprofen at various concentrations were noted in Figure 6 and Table S2, respectively. The results revealed a distinct trend of increasing removal efficiency with higher initial concentrations across all concentrations. However, the efficiency varied remarkably among different concentrations. Notably, the adsorbent BPB600 exhibited lower removal efficiencies compared to other adsorbents, with fluctuations observed at higher concentrations, suggesting the possibility of saturation effects. Among the considered adsorbents, BPB900 (69.28%) showed the highest removal efficiency, followed by BPB800 (67.16%), BPB700 (62.33%), and BPB600 (52.78%) in sequence. This can be ascribed to the greater surface area, pore space, and functional group content mentioned in Figures 2 and 4. As a smoother and more homogeneous surface was produced with increasing pyrolysis temperature, the highest removal efficiency was reported from BPB900. Additionally, no new functional groups were formed at higher pyrolysis temperatures; therefore, the increased removal efficiency might be owing to the greater surface area of the adsorbent (BPB900). This result is comparable with the findings of Patel et al. [30], who opined the increased adsorption capacity for ciprofloxacin and acetaminophen with increasing initial concentration using banana peel biochars (BPBC750). Similarly, biochar derived from pepper stems, pine wood, and wood chips performed efficiently in removing ibuprofen from wastewater, as reported by Naima et al. [34], Essandoh et al. [35], and Lou et al. [63], respectively. The comparative removal efficiency with other adsorbents against ibuprofen or other contaminants was noted in Table 1.

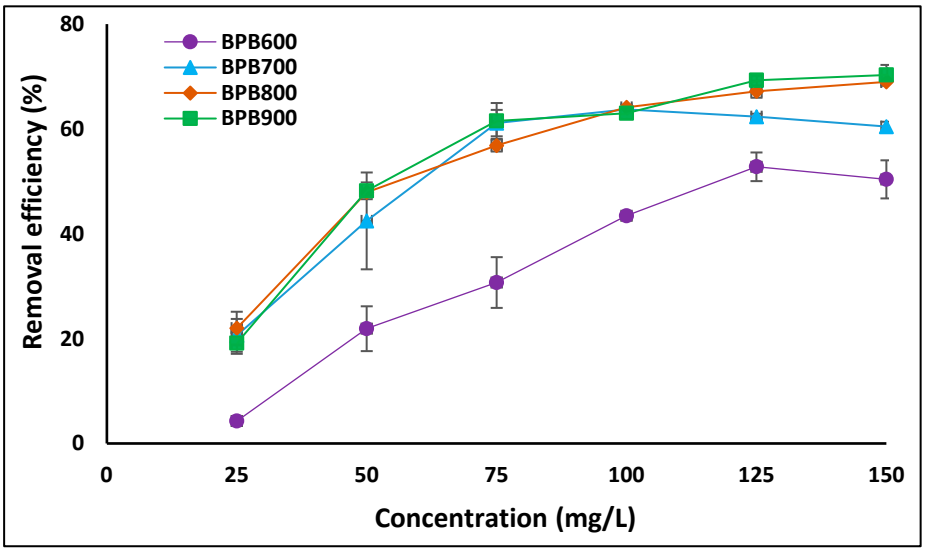


Figure 6. Effect of initial concentrations on the removal efficiency.

Table 1. Comparative table of the previous research.

Serial	Adsorbents	Pollutants	Removal Efficiency (%)	References
1.	*Tamarindus indica* seed biochar	Ibuprofen	91.09	[64]
2.	Activated walnut shell biochar	Ibuprofen	80.00	[36]
3.	Sunflower (*Helianthus annuus*) seed shell biochar	Ibuprofen	34.00	[65]
4.	Olive stones biochar	Diclofenac Ciprofloxacin	87.83 86.41	[66]
5.	Magnetic bio graphene of banana peel biochar	Erythromycin	90.00	[67]
6.	Banana Peel biochar	Ciprofloxacin Acetaminophen	95.00 95.10	[30]
7.	Banana peel biochar	Amoxicillin Carbamazepine	99.43 90.54	[68]
8.	Banana peel biochar	Ibuprofen	70.30	This study

3.3. Adsorption Isotherms

The experimental results were analyzed using two isotherm models, Langmuir and Freundlich, with the results displayed in Figure S1. The Langmuir model showed a weaker fit for the tested adsorbents, with lower R^2 values of 0.8860 (BPB600), 0.6832 (BPB600), 0.7783 (BPB600), and 0.7591 (BPB600), respectively. In contrast, the Freundlich model provided a superior fit, reflected by higher R^2 values of 0.9620, 0.7566, 0.9266, and 0.8844 for BPB600, BPB700, BPB800, and BPB900, respectively. Additionally, a higher n value (less than 1) was observed, indicating a favorable adsorption process where adsorption becomes more linear, suggesting that solute concentration has less influence on adsorption behavior relative to other adsorbents [69]. This heterogeneous system aligns with the Freundlich isotherm, showcasing improved adsorption capacity in a multilayer function [70]. Islam et al. [41] also mentioned a similar finding when performing adsorption of ciprofloxacin using pyrolyzed eggshells.

3.4. Effect of Contact Time on the Removal Efficiency

The relation between shaking time and the removal efficiency of ibuprofen with 125 mg/L against 20 mg BPB900 adsorbent is mentioned in Figure 7. The results illustrated

that there is a rapid increase in ibuprofen removal from 30 to 60 min, where efficiency peaks at 68.17%. However, beyond this point, efficiency begins to increase gradually, reaching its saturation with a removal efficiency of 71.37%. The increasing pattern is assigned to the abundance of easily accessible active sites on adsorbent banana peel biochar surface. After 60 min, the active sites become saturated, resulting in the adsorption reaching equilibrium. An almost similar interaction pattern was observed during the adsorption of ciprofloxacin by pyrolyzed eggshell [41] and eosin dye using Date Palm Carbon Nanofibers by Alminderej et al. [71], respectively.

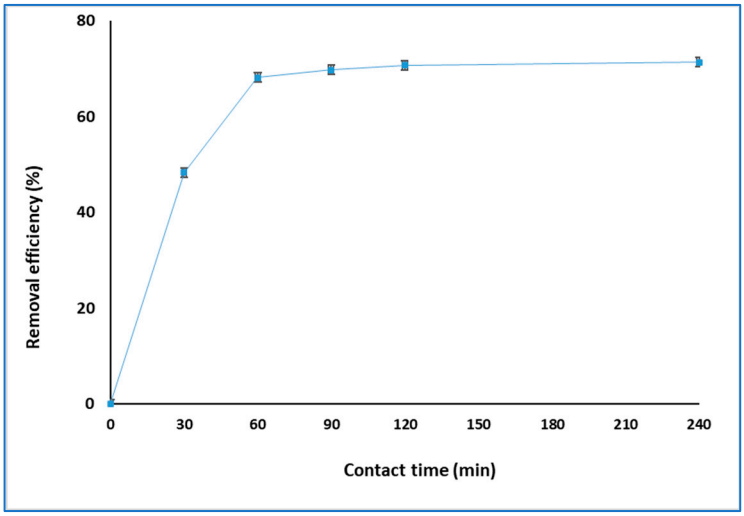


Figure 7. Effect of contact time on the removal efficiency.

3.5. Kinetic Models

The kinetic models (PFO and PSO) of the ibuprofen absorption with banana peel biochar are illustrated in Figure 8. The figure mentioned that the data lack a good fit with the PFO model, as denoted by the lower regression coefficient (R^2: 0.6573). On the other hand, the data show the best fit with the PSO model, with a higher regression coefficient of 0.9969. This suggests that the rate-limiting step governs pollutant removal through the formation of strong chemical bonds, indicating that the interaction between banana peel biochar and ibuprofen is predominantly driven by chemical interactions. At 30 min, the t/qt is approximately 9.93, steadily increasing with longer contact times and reaching around 53.8 at 4 h. The PSO model predominates in the adsorption of ibuprofen, governed by mainly chemical adsorption by the surface of banana peel biochar. This chemisorption process is attributed to the occurrence of functional groups, as stated by Osman et al. [72]. Similar findings were reported by Shin et al. [73] and Reza et al. [74], where they found that the adsorption of ibuprofen was best fitted by PSO with coffee biochar, coconut shell biochar, and bamboo waste biochar, respectively.

3.6. Effects of pH on Removal Efficiency

The effect of pH on the removal efficiency (%) and adsorption rate (mg/g) of ibuprofen is presented in Figure 9. The results indicated that the removal efficiency of ibuprofen exhibits slight variability, ranging between approximately 68% and 73% across the pH spectrum from 3 to 11. Conversely, the adsorption rates remain relatively constant, remaining around 4.4 to 4.5 mg/g across all pH levels. This suggests that while pH levels may marginally influence the removal efficiency of ibuprofen, they have minimal impact on its adsorption onto the BPB900 surface. The adsorption capacity and removal efficiency were influenced by different pH, but it was statistically insignificant. Basically, the pKa of ibuprofen is 4.91 [75]. This indicates that ibuprofen exists in its protonated form (pH < pKa) and deprotonated form (pH > pKa), respectively. On the other hand, the zeta potential of

banana peel biochar (BPB900) was 7.8 (Figure 10), indicating that the surface of BPB900 is negatively charged when pH > pH_{ZPC} and positively charged when pH ≤ pH_{ZPC}.

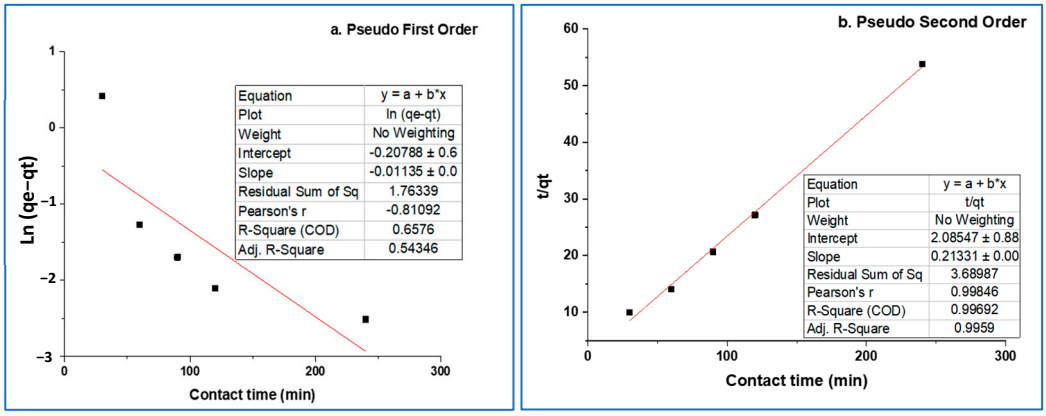


Figure 8. Kinetic models: (**a**) Pseudo First Order (PFO), (**b**) Pseudo Second Order (PSO).

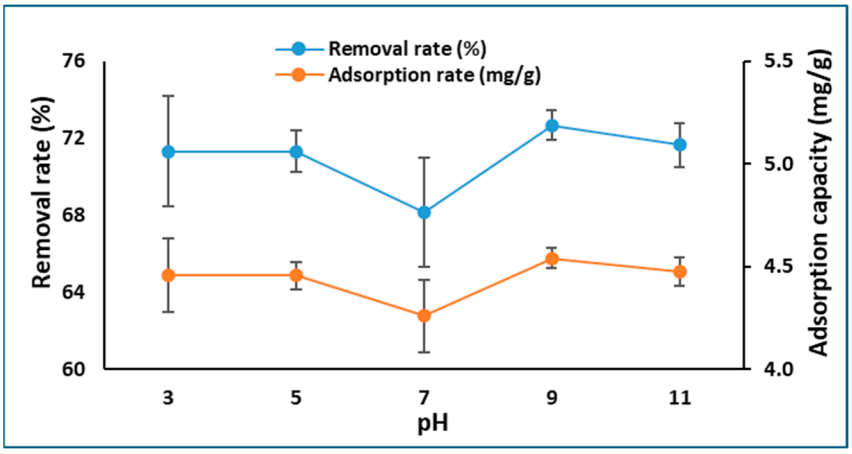


Figure 9. Effect of pH on the removal efficiency and adsorption capacity.

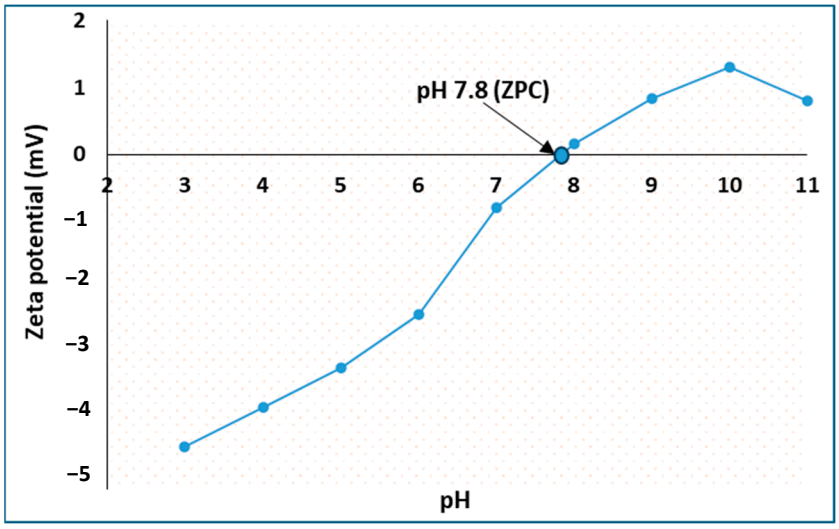


Figure 10. Zeta potential of banana peel biochar (BPB900).

The results mentioned the lowest adsorption at pH 7. At this pH, ibuprofen remains in its deprotonated form (negatively charged), and the adsorbent surface is positively charged (pH ≤ pH_{PZC}), which might promote electrostatic attraction and potentially result

in the highest adsorption. However, the minimum adsorption observed might be due to competition with other negatively charged species (e.g., OH^- ions) or other factors affecting adsorption efficiency. In addition, there might be less overall charge difference between the BPB900 (adsorbent) and ibuprofen, reducing the electrostatic attraction [76].

On the other hand, it was found to have the highest removal performance at pH 9. Although electrostatic repulsion between the BPB900 and the negatively charged ibuprofen at pH 9 could be expected, secondary interactions (hydrogen bonding, van der Waals forces, dipole, and cationic interaction) might act as a driving force that facilitates the adsorption. These results are similar to the results of Patel et al. [4], who explain the hydrogen bonding interaction between the adsorbate and the adsorbent.

3.7. Regeneration Study

The regeneration performance of BPB900 for the adsorption of ibuprofen, as shown in Figure 11, revealed an initial removal efficiency of 69.78% in the first cycle. After four successive regeneration cycles, the removal efficiency was maintained at 58.29%. The reduction in removal efficiency during subsequent regeneration cycles was attributed to surface deformation and material leaching. These results highlight the adsorbent's high effectiveness, cost-efficiency, and environmental friendliness. They further demonstrate that biochar exhibits substantial removal efficiency and reusability for ibuprofen adsorption, suggesting its potential as a viable adsorbent for removing ibuprofen from wastewater. These findings are consistent with those of Yudha et al. [43], who examined the regeneration of HC-12 with RhB and ibuprofen. Similarly, Mohadesi et al. [77] reported over 91% ibuprofen removal after five reuses; however, the removal rate decreased to 83% and 71% in the sixth and seventh cycles, respectively, during the photocatalyst recovery process.

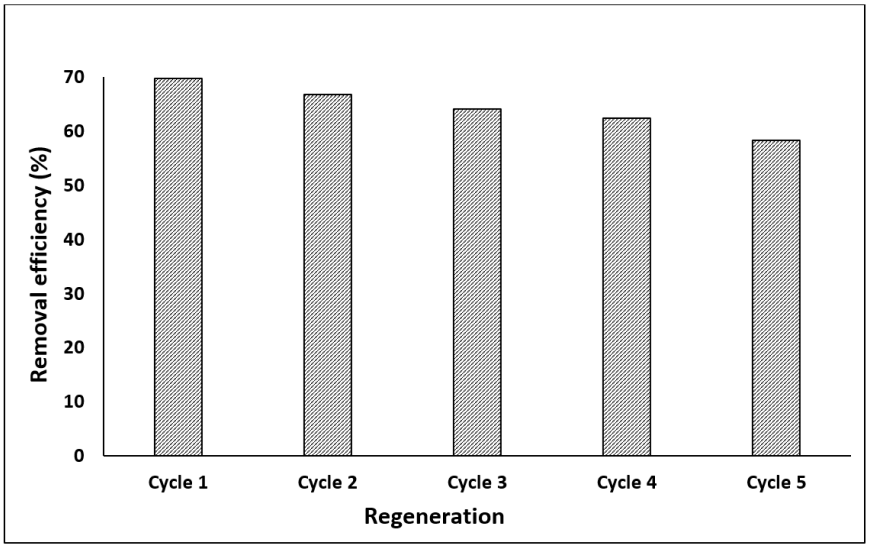


Figure 11. The regeneration performance of BPB900 for the adsorption of ibuprofen.

3.8. Possible Interactions Between Banana Peel Biochar and Ibuprofen

The Fourier Transform Infrared (FTIR) spectra of banana peel biochar reveals distinctive functional groups such as hydroxyl (–OH), carboxyl (COOH), carbonyl (C=O), and aromatic rings (C=C) representing cyclic acid and phenol compound, respectively. Furthermore, the BPB contains several elements, including Ca, Mg, K, and Si, among others, as mentioned in the XPS analysis. Specifically, the carboxylic groups present in banana peel biochar exhibit dual roles as both hydrogen bond donors and acceptors, establishing hydrogen bonds with neutral ibuprofen (pH > 4.91) mentioned in Figure 12. Moreover, the phenolic groups within banana peel biochar, acting as hydrogen bond donors, engage in interactions with deprotonated ibuprofen, which functions as a hydrogen bond acceptor. This interplay is characterized by the phenolic groups of banana peel biochar, which can act

as both hydrogen bond donors and acceptors, engaging in interactions with deprotonated ibuprofen, which similarly participates as both a donor and acceptor of hydrogen bonds. Meanwhile, the carboxylic groups of banana peel biochar primarily function as hydrogen bond acceptors, forming interactions with neutral ibuprofen molecules, which serve as hydrogen bond donors (pH < 4.91). The result was similar to the finding of Patel et al. [30], who reported chemical interactions with the biochar and CIP. In addition, ionic and dipole interaction was observed due to the presence of ions, especially bivalency cations and the polar nature of the functional groups, respectively.

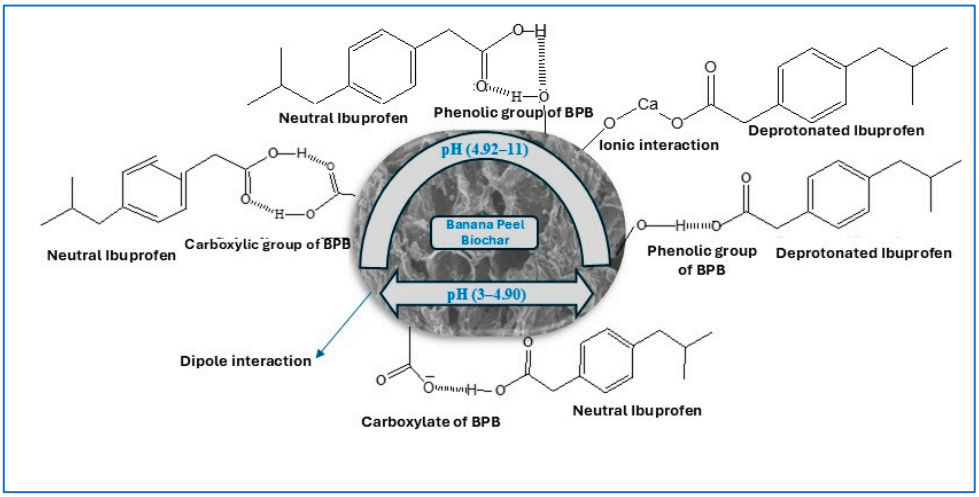


Figure 12. Proposed interactions between banana peel biochar and ibuprofen.

3.9. Evaluation of Machine Learning Algorithms

The results mention the evaluation metrics for five different machine learning regressor algorithms, including Accuracy (%), Standard Deviation, Root Mean Squared Error (RMSE), Mean Absolute Error (MAE), Mean Squared Error (MSE), and R^2 value. Machine learning algorithms are considered superior to simple statistical analysis because they effectively identify patterns and make predictions from data while adapting to complex relationships without relying on strict assumptions. The Random Forest model achieves a remarkable accuracy of 88.79%, with a low standard deviation of 5.94, indicating consistent results (Table 2). It also excels in error metrics, having the lowest MAE, MSE, and RMSE, which collectively suggest high precision and minimal error. Furthermore, the RF model's R^2 score of 0.91 suggests a very good fit for the data. Comparatively, other models exhibit varied performance. The k-NN and DT algorithms perform consistently with good accuracy and low error metrics despite a high standard deviation. The SVM, while having competitive accuracy, has higher error metrics and a lower R^2 score, indicating weaker performance. The LR has moderate accuracy and higher error metrics, indicating less precise predictions. Overall, the dataset demonstrates strong performance across several machine learning algorithms, with the RF algorithm directing in terms of accuracy and predictive quality. Enyoh and Wang [69] noted that RF, DT, and k-NN demonstrated the best performance in classifying aged and undegraded PET MPs.

Table 2. Comparison among different machine learning algorithms.

Machine Learning Algorithm	Accuracy (%)	Standard Deviation	Mean Absolute Error (MAE)	Mean Squared Error (MSE)	Root Mean Squared Error (RMSE)	R^2
LR	74.85	11.02	0.107	0.022	0.148	0.55
SVM	75.79	9.32	0.104	0.023	0.151	0.53
DT	78.82	9.71	0.087	0.015	0.121	0.70
k-NN	80.04	7.47	0.054	0.005	0.072	0.89
RF	88.79	5.94	0.045	0.004	0.066	0.91

The algorithm's ability to handle many features effectively, manage missing values, and provide estimates of feature importance also contributes to its high accuracy. Moreover, RF is less sensitive to hyperparameter tuning compared to some other algorithms, making them easier to implement successfully. This ensemble method handles large feature sets, manages missing values, and highlights feature importance, contributing to its robust and stable predictive performance (Figure 13). This suggests that the data may have a more complex, non-linear pattern that linear regression cannot adequately algorithm, leading to poor predictive accuracy and high errors. Thus, while RF excels in predictive power, DT and k-NN offer more consistent and reliable performance, and LR and SVM are less effective.

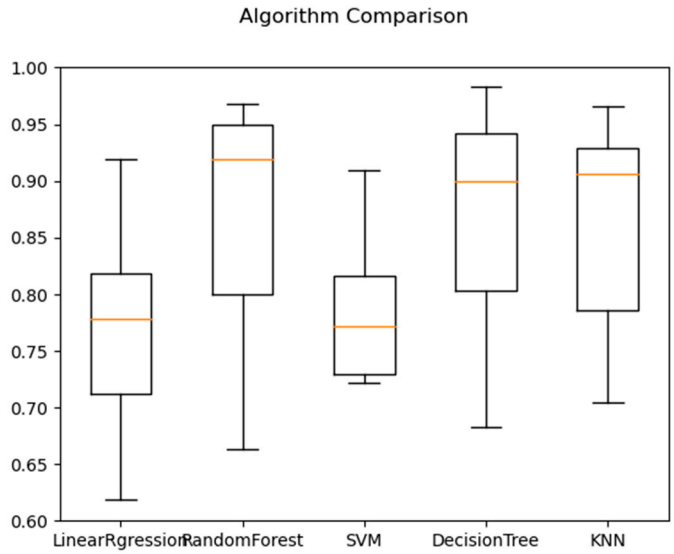


Figure 13. Comparison among different machine learning algorithms.

4. Conclusions

In this research, batch adsorption experiments were performed to investigate the effects of environmental components such as initial ibuprofen concentrations, pH, and contact time on the adsorption. Additionally, LR, RF, SVM, DT, and k-NN—machine learning algorithms were evaluated. The banana peel biochar was prepared at 600, 700, 800, and 900 °C pyrolysis temperatures as adsorbents. The adsorbent was found to have a higher surface area when the pyrolysis temperature increased. The adsorbents contained different functional groups like C=C, CH_2, COOH, phenolic group, and a few metals. The study found that initial concentrations significantly affected ibuprofen removal efficiency with a maximum of 69.28 ± 0.83% against 125 mg/L, with pH also playing a role. The Freundlich adsorption isotherm model was found to be best fitted, having a high R^2 value (0.9620), whereas kinetic analysis demonstrated the applicability of the PSO model (R^2 value 0.9969), revealing complex interactions between banana peel biochar and ibuprofen. Among the algorithms, RF, DT, and k-NN demonstrated superior accuracy, indicating their effectiveness in predicting the adsorption process compared to other batch factors. These findings have significant implications for addressing water pollution caused by pharmaceutical contaminants like ibuprofen and suggest a sustainable and effective approach to water treatment. Future ibuprofen research should emphasize increasing sample size, optimizing biochar properties, and scaling for real-world applications to enhance environmental applicability and predictive accuracy.

Supplementary Materials: The following supporting information can be downloaded at https://www.mdpi.com/article/10.3390/w16233469/s1, Figure S1: Langmuir isotherm (a. BPB600, b. BPB700, c. BPB800, d. BPB00), and Freundlich isotherm (e. BPB600, f. BPB700, g. BPB900), respectively; Table S1: Porous properties of banana peel biochar; Table S2: Adsorption capacity of ibuprofen by banana peel biochar.

Author Contributions: M.R.I.: Conceptualization, Methodology, Investigation, Data curation, Formal analysis, Writing—Original Draft preparation, Q.W.: Supervision, Writing—Original Draft preparation, Review & Editing. S.S.: Methodology, Writing—Original Draft preparation, Review and Editing, C.E.E.: Methodology, Review and Editing. All authors have read and agreed to the published version of the manuscript.

Funding: This study was partially supported by the Special Funds for Innovative Area Research (No. 20120015, FY2008-FY2012) and Basic Research (B) (No. 24310005, FY2012-FY2014; No. 18H03384, FY2017-FY2020; No. 22H03747, FY2022-FY2024) of Grant-in-Aid for Scientific Research of Japanese Ministry of Education, Culture, Sports, Science and Technology (MEXT).

Institutional Review Board Statement: Not applicable.

Informed Consent Statement: Not applicable.

Data Availability Statement: The data are available on request from the corresponding author.

Conflicts of Interest: The authors declare no conflicts of interest.

References

1. Madhav, S.; Bhardwaj, A.K.; Valsami-Jones, E.; Srivastav, A.L. *Urban Water Crisis and Management: Strategies for Sustainable Development*; Elsevier: Amsterdam, The Netherlands, 2022.
2. Gahrouei, A.E.; Vakili, S.; Zandifar, A.; Pourebrahimi, S. From wastewater to clean water: Recent advances on the removal of metronidazole, ciprofloxacin, and sulfamethoxazole antibiotics from water through adsorption and advanced oxidation processes (AOPs). *Environ. Res.* **2024**, *252*, 119029. [CrossRef] [PubMed]
3. Hossain, A.; Nakamichi, S.; Mamun, H.A.; Tani, K.; Masunaga, S.; Matsuda, H. Occurrence and ecological risk of pharmaceuticals in river surface water of Bangladesh. *Environ. Res.* **2018**, *165*, 258–266. [CrossRef] [PubMed]
4. Patel, N.; Khan, Z.A.; Shahane, S.; Rai, D.; Chauhan, D.; Kant, C.; Chaudhary, V.K. Emerging pollutants in aquatic environment: Source, effect, and challenges in biomonitoring and bioremediation—A review. *Pollution* **2020**, *6*, 99–113.
5. Shaheen, J.F.; Eniola, J.O.; Sizirici, B. Adsorption of ibuprofen from aqueous solution by modified date palm biochar: Performance, optimization, and life cycle assessment. *Bioresour. Technol. Rep.* **2024**, *25*, 101696. [CrossRef]
6. Chopra, S.; Kumar, D. Ibuprofen as an emerging organic contaminant in environment, distribution and remediation. *Heliyon* **2020**, *6*, e04087. [CrossRef]
7. Guedidi, H.; Belkacemi, M.; Chebbi, A.; Mhenni, M.F.; Ghorbel, A.; Bousselmi, L. Removal of ionic liquids and ibuprofen by adsorption on a microporous activated carbon: Kinetics, isotherms, and pore sites. *Arab. J. Chem.* **2020**, *13*, 258–270. [CrossRef]
8. Letsoalo, M.R.; Sithole, T.; Mufamadi, S.; Mazhandu, Z.; Sillanpaa, M.; Kaushik, A.; Mashifana, T. Efficient detection and treatment of pharmaceutical contaminants to produce clean water for better health and environmental. *J. Clean. Prod.* **2023**, *387*, 135798. [CrossRef]
9. Ellepola, N.; Ogas, T.; Turner, D.N.; Gurung, R.; Maldonado-Torres, S.; Tello-Aburto, R.; Patidar, P.L.; Rogelj, S.; Piyasena, M.E.; Rubasinghege, G. A toxicological study on photo-degradation products of environmental ibuprofen: Ecological and human health implications. *Ecotoxicol. Environ. Saf.* **2020**, *188*, 109892. [CrossRef]
10. Mazaleuskaya, L.L.; Theken, K.N.; Gong, L.; Thorn, C.F.; FitzGerald, G.A.; Altman, R.B.; Klein, T.E. PharmGKB summary: Ibuprofen pathways. *Pharmacogenet. Genom.* **2015**, *25*, 96–106. [CrossRef]
11. Xing, T.; Wu, Y.; Wang, Q.; Sadrnia, A.; Behmaneshfar, A.; Dragoi, E.N. Adsorption of ibuprofen using waste coffee derived carbon architecture: Experimental, kinetic modeling, statistical and bio-inspired optimization. *Environ. Res.* **2023**, *231*, 116223. [CrossRef]
12. Thabede, P.M.; Mtunzi, F.; Nyamukamba, P. Sorption behaviour of ibuprofen using activated carbon derived from rose geranium (*Pelargonium graveolens* L.) leaves. *Appl. Sci.* **2023**, *13*, 5133. [CrossRef]
13. Zhang, Q.; Ye, X.; Li, H.; Chen, D.; Xiao, W.; Zhao, S.; Xiong, R.; Li, J. Cumulative effects of pyrolysis temperature and process on properties, chemical speciation, and environmental risks of heavy metals in magnetic biochar derived from coagulation-flocculation sludge of swine wastewater. *J. Environ. Chem. Eng.* **2020**, *8*, 104472. [CrossRef]
14. Carolin, C.F.; Kumar, P.S.; Joshiba, G.J.; Kumar, V.V. Analysis and removal of pharmaceutical residues from wastewater using membrane bioreactors: A review. *Environ. Chem. Lett.* **2021**, *19*, 329–343. [CrossRef]
15. Wu, J.; Wang, T.; Wang, J.; Zhang, Y.; Pan, W.P. A novel modified method for the efficient removal of Pb and Cd from wastewater by biochar: Enhanced ion exchange and precipitation capacity. *Sci. Total Environ.* **2021**, *754*, 142150. [CrossRef]
16. Liu, W.; Wu, Y.; Yi, G.; Guo, X.; Yin, Y.; Xu, B.; Zhou, J.; Li, Q.; Zhang, Y. Carbonized nitrogen-doped carbon dots functionalized PbO_2 electrode for efficient degradation of organic pollutants. *J. Mol. Struct.* **2025**, *1319*, 139453. [CrossRef]
17. Devi, P.; Das, U.; Dalai, A.K. In-situ chemical oxidation: Principle and applications of peroxide and persulfate treatments in wastewater systems. *Sci. Total Environ.* **2016**, *571*, 643–657. [CrossRef]

18. Saeid, S.; Tolvanen, P.; Kumar, N.; Eränen, K.; Peltonen, J.; Peurla, M.; Mikkola, J.P.; Franz, A.; Salmi, T. Advanced oxidation process for the removal of ibuprofen from aqueous solution: A non-catalytic and catalytic ozonation study in a semi-batch reactor. *Appl. Catal. B Environ.* **2018**, *230*, 77–90. [CrossRef]
19. Hoseinzadeh, E.; Rezaee, A.; Hossini, H. Biological nitrogen removal in moving bed biofilm reactor using ibuprofen as carbon source. *Water Air Soil Pollut.* **2016**, *227*, 46. [CrossRef]
20. Chen, Y.; Luo, W.; Meng, F.; Zhou, T.; Lai, F.; Zhao, Z.; Liu, Y.; Li, J. Sustainable application study of disposable medical waste masks in cement based on green Fenton reaction. *J. Appl. Polym. Sci.* **2024**, *141*, e55049. [CrossRef]
21. Varela, C.F.; Moreno-Aldana, L.C.; Agámez-Pertuz, Y.Y. Adsorption of pharmaceutical pollutants on $ZnCl_2$-activated biochar from corn cob: Efficiency, selectivity and mechanism. *J. Bioresour. Bioprod.* **2024**, *9*, 58–73. [CrossRef]
22. Satyam, S.; Patra, S. Innovations and challenges in adsorption-based wastewater remediation: A comprehensive review. *Helion* **2024**, *10*, e29573. [CrossRef] [PubMed]
23. Zamani, S.A.; Yunus, R.; Samsuri, A.W.; Salleh, M.M.; Asady, B. Removal of zinc from aqueous solution by optimized oil palm empty fruit bunches biochar as low cost adsorbent. *Bioinorg. Chem. Appl.* **2017**, *2017*, 7914714. [CrossRef] [PubMed]
24. Mansouri, F.; Chouchene, K.; Wali, A.; Labille, J.; Roche, N.; Ksibi, M. Adsorption of anti-inflammatory and analgesic drugs traces in water on clay minerals. *Chemosphere* **2024**, *353*, 141469. [CrossRef] [PubMed]
25. FAO. Banana Market Review 2022, Rome. 2023. Available online: https://openknowledge.fao.org/server/api/core/bitstreams/cd3e1df8-6e70-461a-9963-9827ad69389f/content (accessed on 28 September 2024).
26. Singh, S.; Parveen, N.; Gupta, H. Adsorptive decontamination of rhodamine-B from water using banana peel powder: A biosorbent. *Environ. Technol. Innov.* **2018**, *12*, 189–195. [CrossRef]
27. Lotfabad, E.M.; Ding, J.; Cui, K.; Kohandehghan, A.; Kalisvaart, W.P.; Hazelton, M.; Mitlin, D. High-density sodium and lithium ion battery anodes from banana peels. *ACS Nano* **2014**, *8*, 7115–7129. [CrossRef]
28. Pathak, P.D.; Mandavgane, S.A. Preparation and characterization of raw and carbon from banana peel by microwave activation: Application in citric acid adsorption. *J. Environ. Chem. Eng.* **2015**, *3*, 2435–2447. [CrossRef]
29. ul Haq, A.; Shah, J.; Jan, M.R.; ud Din, S. Kinetic, equilibrium and thermodynamic studies for the sorption of metribuzin from aqueous solution using banana peels, an agro-based biomass. *Toxicol. Environ. Chem.* **2015**, *97*, 124–134. [CrossRef]
30. Patel, M.; Kumar, R.; Pittman, C.U., Jr.; Mohan, D. Ciprofloxacin and acetaminophen sorption onto banana peel biochars: Environmental and process parameter influences. *Environ. Res.* **2021**, *201*, 111218. [CrossRef]
31. Akpomie, K.G.; Conradie, J. Banana peel as a biosorbent for the decontamination of water pollutants: A review. *Environ. Chem. Lett.* **2020**, *18*, 1085–1112. [CrossRef]
32. Ighalo, J.O.; Conradie, J.; Ohoro, C.R.; Amaku, J.F.; Oyedotun, K.O.; Maxakato, N.W.; Akpomie, K.G.; Okeke, E.S.; Olisah, C.; Malloum, A.; et al. Biochar from coconut residues: An overview of production, properties, and applications. *Ind. Crops Prod.* **2023**, *204*, 117300. [CrossRef]
33. Yang, X.; Zhang, X.; Ngo, H.H.; Guo, W.; Huo, J.; Du, Q.; Zhang, Y.; Li, C.; Yang, F. Sorptive removal of ibuprofen from water by natural porous biochar derived from recyclable plane tree leaf waste. *J. Water Process Eng.* **2022**, *46*, 102627. [CrossRef]
34. Naima, A.; Ammar, F.; Abdelkader, O.; Rachid, C.; Lynda, H.; Syafiuddin, A.; Boopathy, R. Development of a novel and efficient biochar produced from pepper stem for effective ibuprofen removal. *Bioresour. Technol.* **2022**, *347*, 126685. [CrossRef] [PubMed]
35. Essandoh, M.; Kunwar, B.; Pittman, C.U., Jr.; Mohan, D.; Mlsna, T. Sorptive removal of salicylic acid and ibuprofen from aqueous solutions using pine wood fast pyrolysis biochar. *Chem. Eng. J.* **2015**, *265*, 219–227. [CrossRef]
36. Patel, M.; Chaubey, A.K.; Pittman, C.U., Jr.; Mohan, D. Aqueous ibuprofen sorption by using activated walnut shell biochar: Process optimization and cost estimation. *Environ. Sci. Adv.* **2022**, *1*, 530–545. [CrossRef]
37. Montgomery, D.C.; Peck, E.A.; Vining, G.G. *Introduction to Linear Regression Analysis*; John Wiley & Sons: Hoboken, NJ, USA, 2021.
38. Gawade, P.; Nandi, S.; Meena, C.; Sarkar, R.R. Artificial intelligence and machine learning techniques using omics data for cancer diagnosis and treatment. In *Systems Biomedicine Approaches in Cancer Research*; Springer Nature: Singapore, 2022; pp. 23–50. [CrossRef]
39. Rigatti, S.J. Random forest. *J. Insur. Med.* **2017**, *47*, 31–39. [CrossRef]
40. Islam, M.R.; Wang, Q.; Guo, Y.; Wang, W.; Sharmin, S.; Enyoh, C.E. Physico-chemical characterization of food wastes for potential soil application. *Processes* **2023**, *11*, 250. [CrossRef]
41. Islam, M.R.; Wang, Q.; Sharmin, S.; Wang, W. Exploring the efficacy of eggshell and its pyrolyzed products for ciprofloxacin removal with machine learning insights. *Chem. Pap.* **2024**, *78*, 8433–8447. [CrossRef]
42. Awual, M.E.; Salman, M.S.; Hasan, M.M.; Hasan, M.N.; Kubra, K.T.; Sheikh, M.C.; Rasee, A.I.; Rehan, A.I.; Waliullah, R.M.; Hossain, M.S.; et al. Ligand imprinted composite adsorbent for effective Ni (II) ion monitoring and removal from contaminated water. *J. Ind. Eng. Chem.* **2024**, *131*, 585–592. [CrossRef]
43. Yudha, S.P.; Tekasakul, S.; Phoungthong, K.; Chuenchom, L. Green synthesis of low-cost and eco-friendly adsorbent for dye and pharmaceutical adsorption: Kinetic, isotherm, thermodynamic and regeneration studies. *Mater. Res. Express* **2019**, *6*, 125526. [CrossRef]
44. Baláž, P.; Aláčová, A.; Briančin, J. Sensitivity of Freundlich equation constant 1/n for zinc sorption on changes induced in calcite by mechanical activation. *Chem. Eng. J.* **2005**, *114*, 115–121. [CrossRef]
45. Liu, Y.; Shen, L. From Langmuir kinetics to first-and second-order rate equations for adsorption. *Langmuir* **2008**, *24*, 11625–11630. [CrossRef]

46. Ho, Y.S.; McKay, G. Pseudo-second order model for sorption processes. *Process Biochem.* **1999**, *34*, 451–465. [CrossRef]
47. Dahiya, N.; Gupta, S.; Singh, S. A review paper on machine learning applications, advantages, and techniques. *ECS Trans.* **2022**, *107*, 6137. [CrossRef]
48. Yin, G.; Alazzawi, F.J.I.; Mironov, S.; Reegu, F.; El-Shafay, A.S.; Rahman, M.L.; Su, C.H.; Lu, Y.Z.; Nguyen, H.C. Machine learning method for simulation of adsorption separation: Comparisons of model's performance in predicting equilibrium concentrations. *Arab. J. Chem.* **2022**, *15*, 103612. [CrossRef]
49. Mahesh, B. Machine learning algorithms—A review. *Int. J. Sci. Res.* **2020**, *9*, 381–386. [CrossRef]
50. Oyekanmi, A.A.; Ahmad, A.; Hossain, K.; Rafatullah, M. Adsorption of Rhodamine B dye from aqueous solution onto acid treated banana peel: Response surface methodology, kinetics and isotherm studies. *PLoS ONE* **2019**, *14*, e0216878. [CrossRef]
51. Shenwari, K.A.; Priyatharshini, S.; Dhevagi, P.; Chitdeshwari, T.; Avudainayagam, S. Removal of Lead and Cadmium from aqueous solutions by Banana Peel Biochar. *Madras Agric. J.* **2019**, *106*, 1–3. [CrossRef]
52. Zubair, M.; Mu'azu, N.D.; Jarrah, N.; Blaisi, N.I.; Aziz, H.A.; Al-Harthi, M.A. Adsorption behavior and mechanism of methylene blue, crystal violet, eriochrome black T, and methyl orange dyes onto biochar-derived date palm fronds waste produced at different pyrolysis conditions. *Water Air Soil Pollut.* **2020**, *231*, 240. [CrossRef]
53. Shah, V.; Soni, V.; Daverey, A. Valorization of banana peel as biochar and assessment of its effect in biochar-assisted phytoremediation of cadmium-contaminated soil by using the Taguchi method. *Biomass Convers. Biorefinery* **2023**, *13*, 9451–9463. [CrossRef]
54. Yazdani, M.R.; Duimovich, N.; Tiraferri, A.; Laurell, P.; Borghei, M.; Zimmerman, J.B.; Vahala, R. Tailored mesoporous biochar sorbents from pinecone biomass for the adsorption of natural organic matter from lake water. *J. Mol. Liq.* **2019**, *291*, 111248. [CrossRef]
55. Qin, Q.; Zhong, F.; Song, T.; Yang, Z.; Zhang, P.; Cao, H.; Yao, Z. Optimization of multiscale structure and electrochemical properties of bamboo-based porous activated biochar by coordinated regulation of activation and air oxidation. *Chem. Eng. J.* **2023**, *477*, 146763. [CrossRef]
56. Gęca, M.; Khalil, A.M.; Tang, M.; Bhakta, A.K.; Snoussi, Y.; Nowicki, P.; Chehimi, M.M. Surface treatment of biochar—Methods, surface analysis and potential applications: A comprehensive review. *Surfaces* **2023**, *6*, 179–213. [CrossRef]
57. Xu, S.; Yu, W.; Liu, S.; Xu, C.; Li, J.; Zhang, Y. Adsorption of hexavalent chromium using banana pseudostem biochar and its mechanism. *Sustainability* **2018**, *10*, 4250. [CrossRef]
58. Nguyen, V.T.; Nguyen, T.B.; Dat, N.D.; Vo, T.K.Q.; Nguyen, X.C.; Dinh, V.C.; Le, T.N.C.; Duong, T.G.H.; Bui, M.H.; Bui, X.T. Preliminary study of doxycycline adsorption from aqueous solution on alkaline modified biochar derived from banana peel. *Environ. Eng. Res.* **2024**, *29*, 230196. [CrossRef]
59. Özçimen, D.; Ersoy-Meriçboyu, A. Characterization of biochar and bio-oil samples obtained from carbonization of various biomass materials. *Renew. Energy* **2010**, *35*, 1319–1324. [CrossRef]
60. Li, G.; Zhu, W.; Zhang, C.; Zhang, S.; Liu, L.; Zhu, L.; Zhao, W. Effect of a magnetic field on the adsorptive removal of methylene blue onto wheat straw biochar. *Bioresour. Technol.* **2016**, *206*, 16–22. [CrossRef]
61. Zhang, Y.; Ruan, K.; Zhou, K.; Gu, J. Controlled distributed Ti_3C_2Tx hollow microspheres on thermally conductive polyimide composite films for excellent electromagnetic interference shielding. *Adv. Mater.* **2023**, *35*, 2211642. [CrossRef]
62. Chen, Y.; Liu, Y.; Li, Y.; Chen, Y.; Wu, Y.; Li, H.; Wang, S.; Peng, Z.; Xu, R.; Zeng, Z. Novel magnetic pomelo peel biochar for enhancing Pb (II) and Cu (II) adsorption: Performance and mechanism. *Water Air Soil Pollut.* **2020**, *231*, 1–15. [CrossRef]
63. Lou, Y.; Tan, F.J.; Zeng, R.; Wang, M.; Li, P.; Xia, S. Preparation of cross-linked graphene oxide on polyethersulfone membrane for pharmaceuticals and personal care products removal. *Polymers* **2020**, *12*, 1921. [CrossRef]
64. Show, S.; Chowdhury, S.; Maji, M.; Sarkar, P.; Ghosh, M.; Sillanpää, M.; Halder, G. Sorptive elimination of ibuprofen using activated biochar: Modelling, non-linear isotherm and kinetic, cost assessment and toxicity analysis. *Biomass Convers. Biorefinery* **2024**, *14*, 11579–11600. [CrossRef]
65. Alvear-Daza, J.J.; Rengifo-Herrera, J.A.; Pizzio, L.R. Performance and optimization of diclofenac and ibuprofen adsorption onto activated carbon synthesized from sunflower seed shell (*Helianthus annuus*) in natural groundwater samples. *Adsorption* **2024**, *30*, 783–800. [CrossRef]
66. Al-Sareji, O.J.; Grmasha, R.A.; Meiczinger, M.; Al-Juboori, R.A.; Somogyi, V.; Hashim, K.S. A sustainable banana peel activated carbon for removing pharmaceutical pollutants from different waters: Production, characterization, and application. *Materials* **2024**, *17*, 1032. [CrossRef] [PubMed]
67. Juela, D.M. Promising adsorptive materials derived from agricultural and industrial wastes for antibiotic removal: A comprehensive review. *Sep. Purif. Technol.* **2022**, *284*, 120286. [CrossRef]
68. Al-Sareji, O.J.; Grmasha, R.A.; Meiczinger, M.; Al-Juboori, R.A.; Somogyi, V.; Stenger-Kovács, C.; Hashim, K.S. A sustainable and highly efficient fossil-free carbon from olive stones for emerging contaminants removal from different water matrices. *Chemosphere* **2024**, *351*, 141189. [CrossRef] [PubMed]
69. Enyoh, C.E.; Wang, Q. Automated classification of undegraded and aged polyethylene terephthalate microplastics from ATR-FTIR spectroscopy using machine learning algorithms. *J. Polym. Environ.* **2024**, *32*, 4143–4158. [CrossRef]
70. Tohamy, H.A.S.; El-Sakhawy, M.; Hassan, E.B.; Kamel, S. Microwave-Prepared Quantum Dots and Their Potential Applications as Adsorbents and Chemosensors. *Materials* **2023**, *16*, 6722. [CrossRef]

71. Alminderej, F.M.; Albadri, A.E.; El-Ghoul, Y.; El-Sayed, W.A.; Younis, A.M.; Saleh, S.M. Sustainable and green synthesis of carbon nanofibers from date palm residues and their adsorption efficiency for eosin dye. *Sustainability* **2023**, *15*, 10451. [CrossRef]
72. Osman, A.I.; Ayati, A.; Farghali, M.; Baghery, S.; Ahmed, A.K.; Karimian, N.; Kumar, P.; Gupta, V.K.; Al-Ahmad, M.; Ali, I.; et al. Advanced adsorbents for ibuprofen removal from aquatic environments: A review. *Environ. Chem. Lett.* **2024**, *22*, 373–418. [CrossRef]
73. Shin, J.; Kwak, J.; Lee, Y.G.; Kim, S.; Choi, M.; Bae, S.; Lee, S.H.; Park, Y.; Chon, K. Competitive adsorption of pharmaceuticals in lake water and wastewater effluent by pristine and NaOH-activated biochars from spent coffee wastes: Contribution of hydrophobic and π–π interactions. *Environ. Pollut.* **2021**, *270*, 116244. [CrossRef]
74. Reza, R.A.; Ahmaruzzaman, M.; Sil, A.K.; Gupta, V.K. Comparative adsorption behavior of Ibuprofen and clofibric acid onto microwave assisted activated bamboo waste. *Ind. Eng. Chem. Res.* **2014**, *53*, 9331–9339. [CrossRef]
75. Lindqvist, N.; Tuhkanen, T.; Kronberg, L. Occurrence of acidic pharmaceuticals in raw and treated sewages and in receiving waters. *Water Res.* **2005**, *39*, 2219–2228. [CrossRef] [PubMed]
76. Oba, S.N.; Ighalo, J.O.; Aniagor, C.O.; Igwegbe, C.A. Removal of ibuprofen from aqueous media by adsorption: A comprehensive review. *Sci. Total Environ.* **2021**, *780*, 146608. [CrossRef] [PubMed]
77. Mohadesi, M.; Gouran, A.; Seifi, K. Removal of ibuprofen from synthetic wastewater using photocatalytic method in the presence of FeO photocatalyst supported on modified Iranian clinoptilolite. *Environ. Sci. Pollut. Res.* **2022**, *29*, 34338–34348. [CrossRef] [PubMed]

Disclaimer/Publisher's Note: The statements, opinions and data contained in all publications are solely those of the individual author(s) and contributor(s) and not of MDPI and/or the editor(s). MDPI and/or the editor(s) disclaim responsibility for any injury to people or property resulting from any ideas, methods, instructions or products referred to in the content.